Supporting Information

Peptide-Directed Assembly of Single-Helical Gold Nanoparticle Superstructures Exhibiting Intense Chiroptical Activity

Andrea D. Merg,[†] *Jennifer C. Boatz*,[‡] *Abhishek Mandal*,[‡] *Gongpu Zhao*,[‡] *Soumitra Mokashi-Punekar*,[†] *Chong Liu*,[†] *Xianting Wang*,[‡] *Peijun Zhang*,[‡] *Patrick C. A. van der Wel*,*[‡] *and Nathaniel L. Rosi**[†]

[†]Department of Chemistry, University of Pittsburgh, 219 Parkman Ave., Pittsburgh, Pennsylvania 15260, United States

[‡]Department of Structural Biology, University of Pittsburgh, School of Medicine, 3501 Fifth Avenue, Pittsburgh, Pennsylvania 15260, United States

Supplementary Data

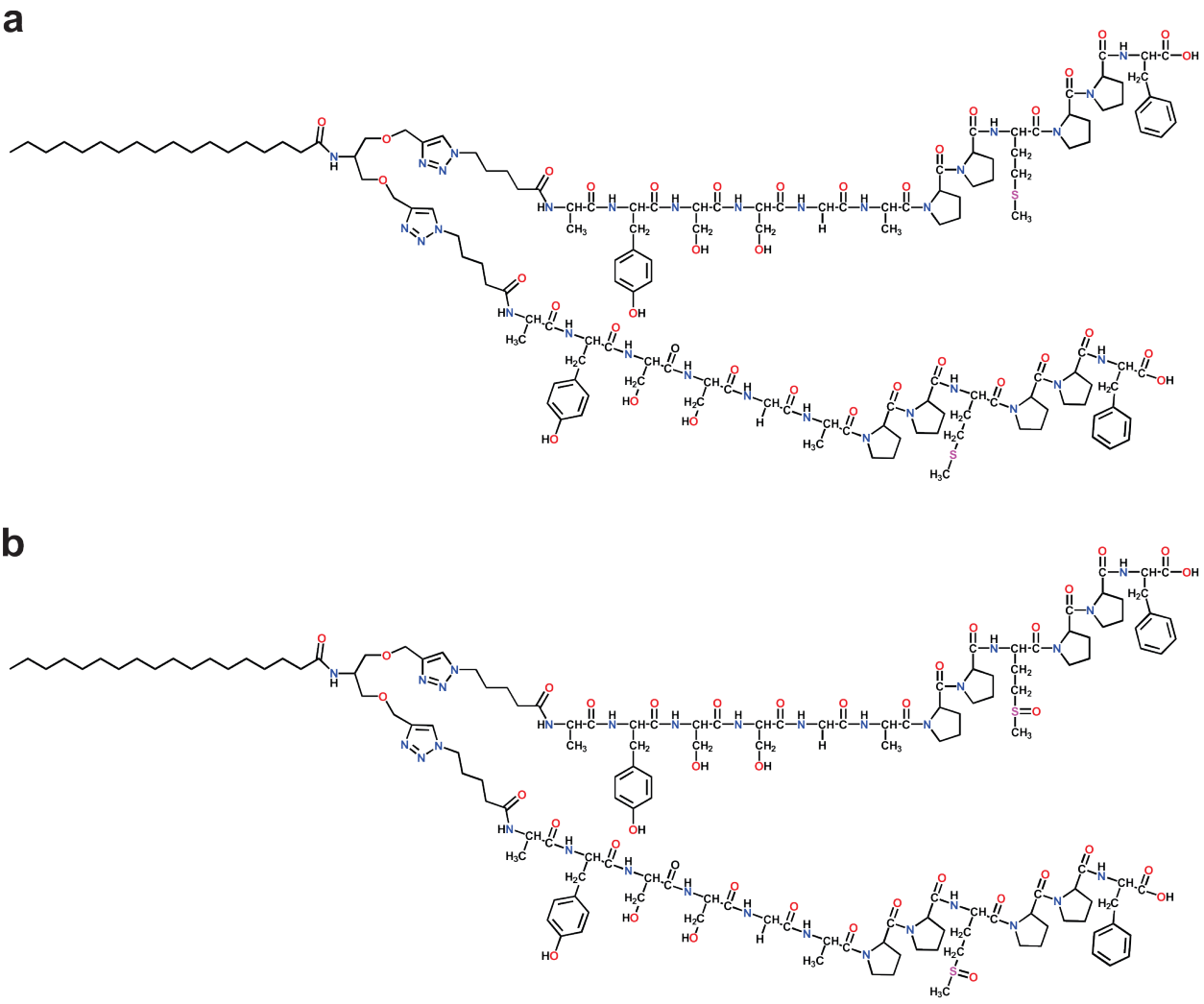

Figure S1. Chemical structure of (a) C_{18}-$(PEP_{Au})_2$ and (b) C_{18}-$(PEP_{Au}{}^{M\text{-}Ox})_2$.

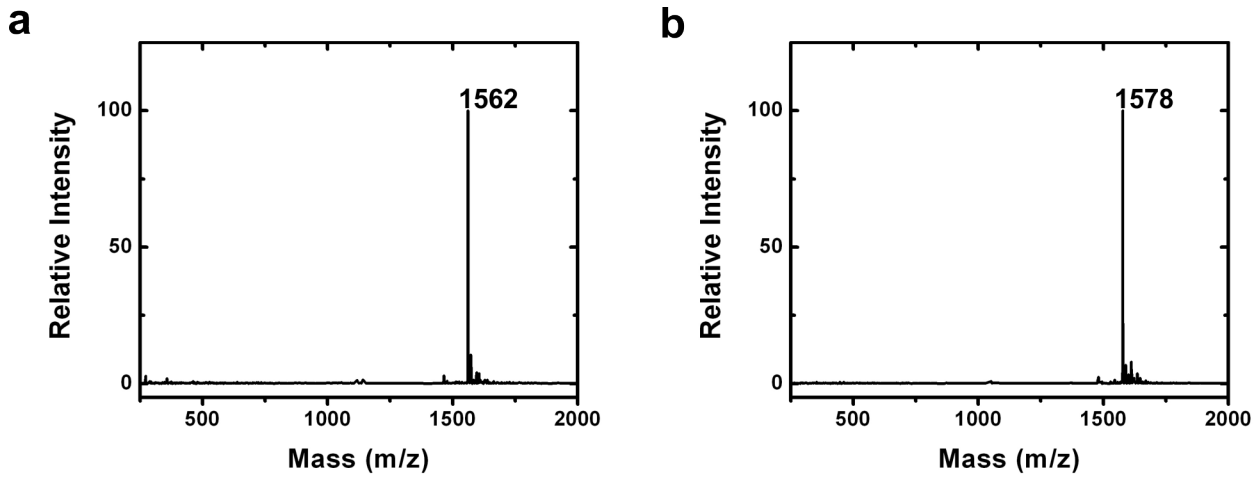

Figure S2. LCMS spectra of (a) C_{18}-$(PEP_{Au})_2$, m/z = 1562 (m/2) and (b) C_{18}-$(PEP_{Au}{}^{M\text{-}Ox})_2$, m/z = 1578 (m/2).

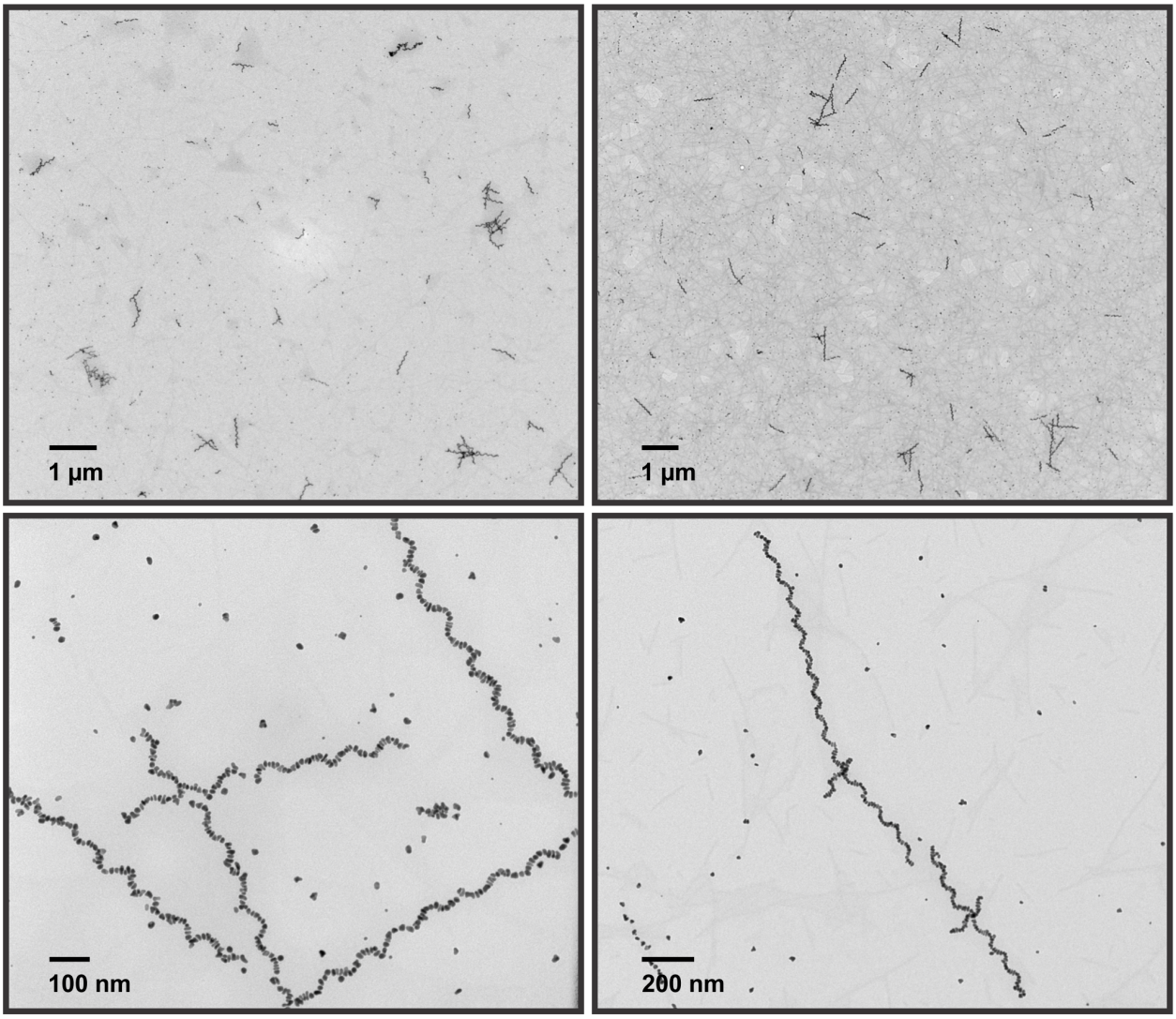

Figure S3. Additional TEM images of the single-helical superstructure at different magnifications.

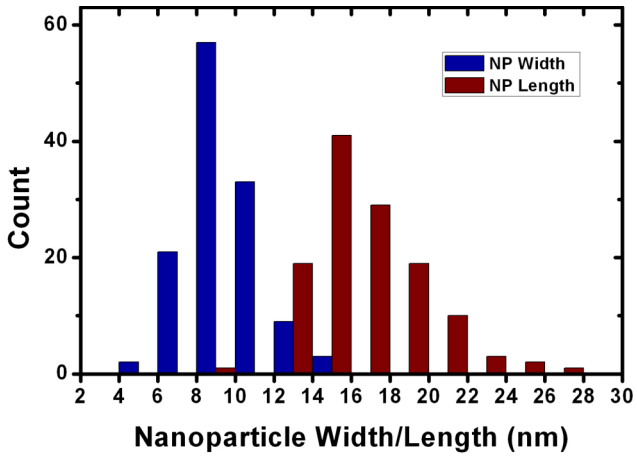

Figure S4. The nanoparticle length and widths of the single-helical superstructure were 16.6 ± 3.0 nm and 9.6 ± 1.9 nm, respectively, after 15 hours of reaction (based on 125 counts each).

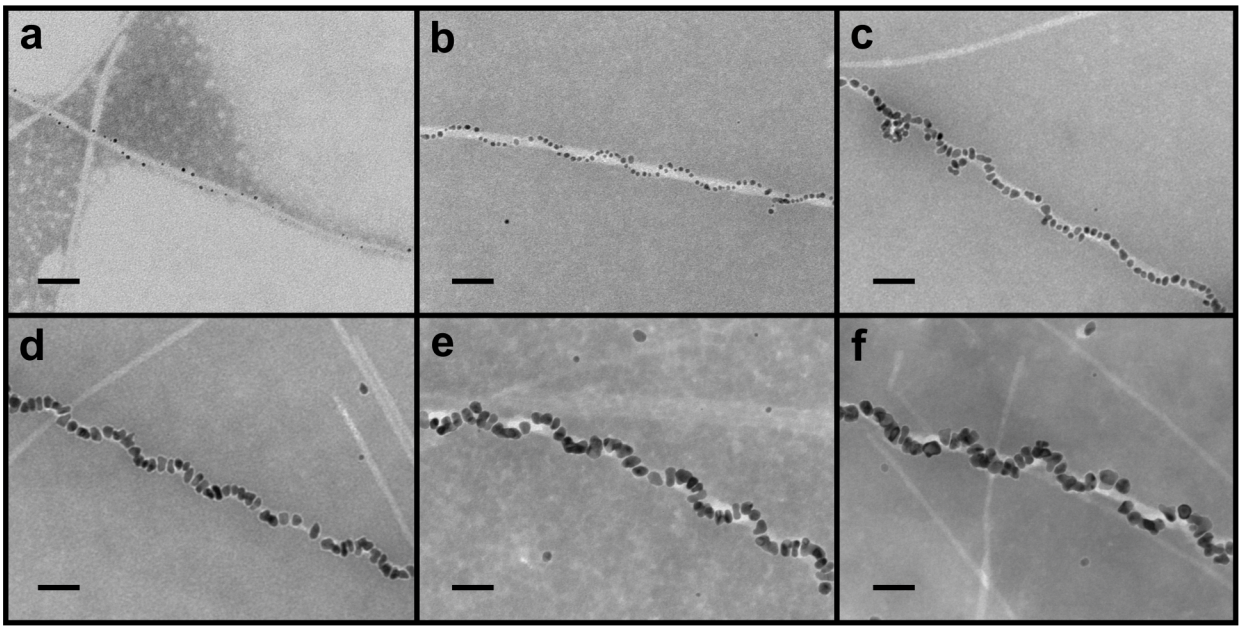

Figure S5. Negative stained TEM images of the single helices after (a) 0 min., (b) 30 min., (c) 2 hrs., (d) 5 hrs., (e) 8 hrs., and (f) 2 days of reaction at room temperature (scale bar = 50 nm).

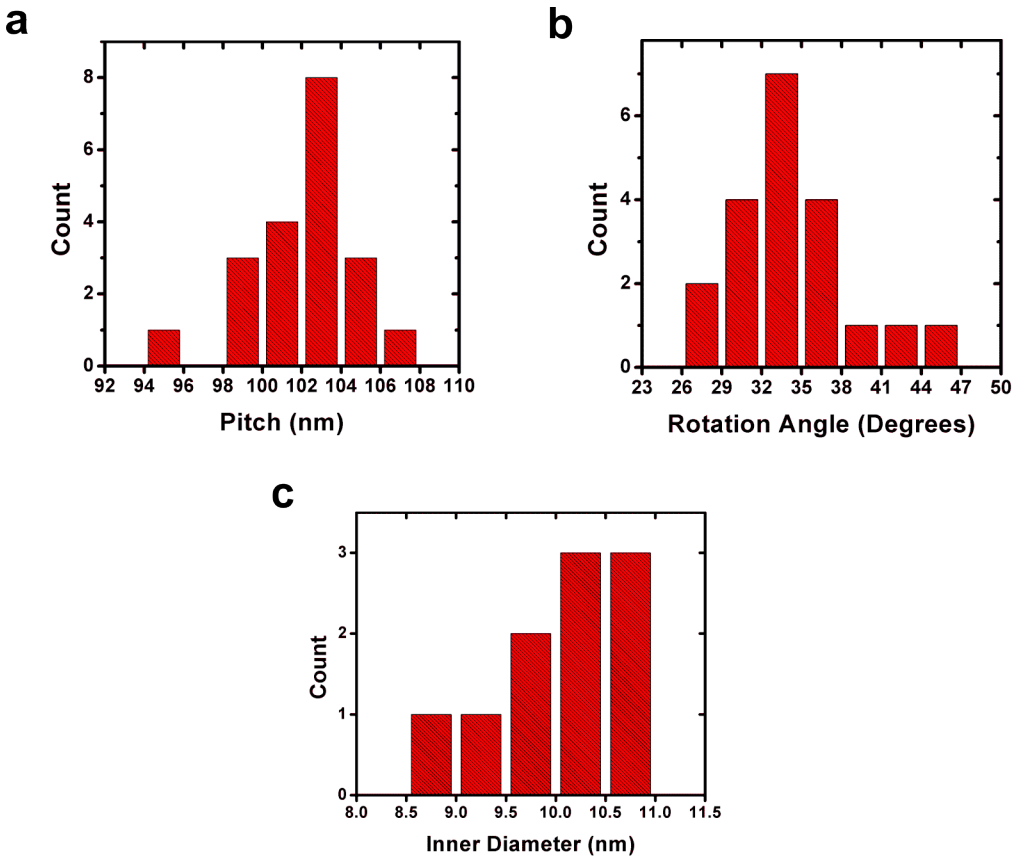

Figure S6. Structural parameters of single helices from cryo-ET: (a) the helical pitch was 102.0 ± 2.5 nm, based on 20 counts; (b) rotation angle was 34.3 ± 4.9 degrees, based on 20 counts; and (c) inner diameter was 10.1 ± 0.6 nm, based on 10 counts.

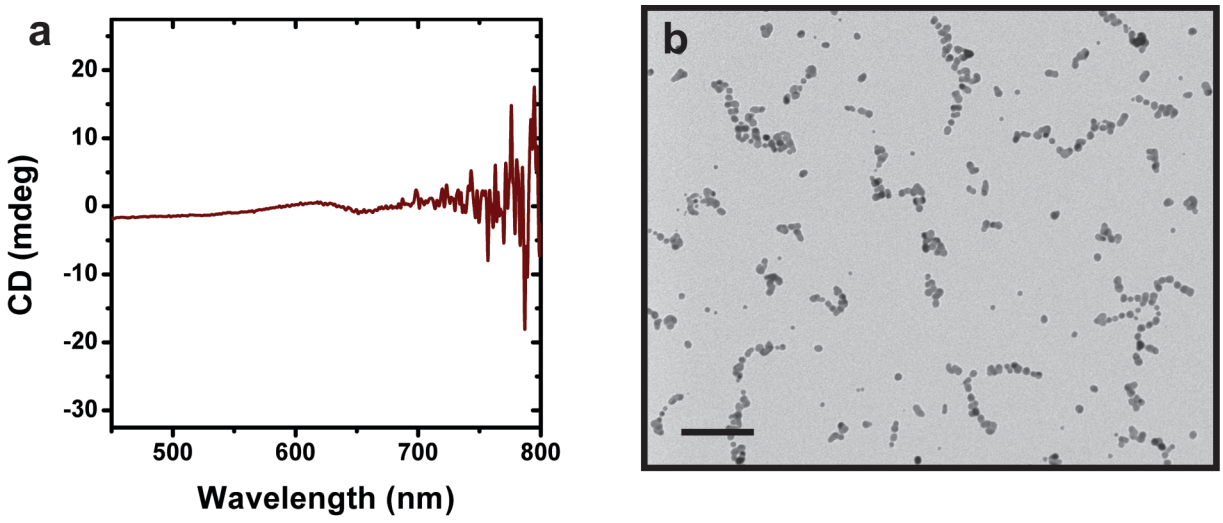

Figure S7. (a) CD spectrum of $PEP_{Au}^{M\text{-}ox}$ capped gold nanoparticles and (b) their corresponding TEM image (scale bar = 100 nm). Both single particles and particle aggregates are observed.

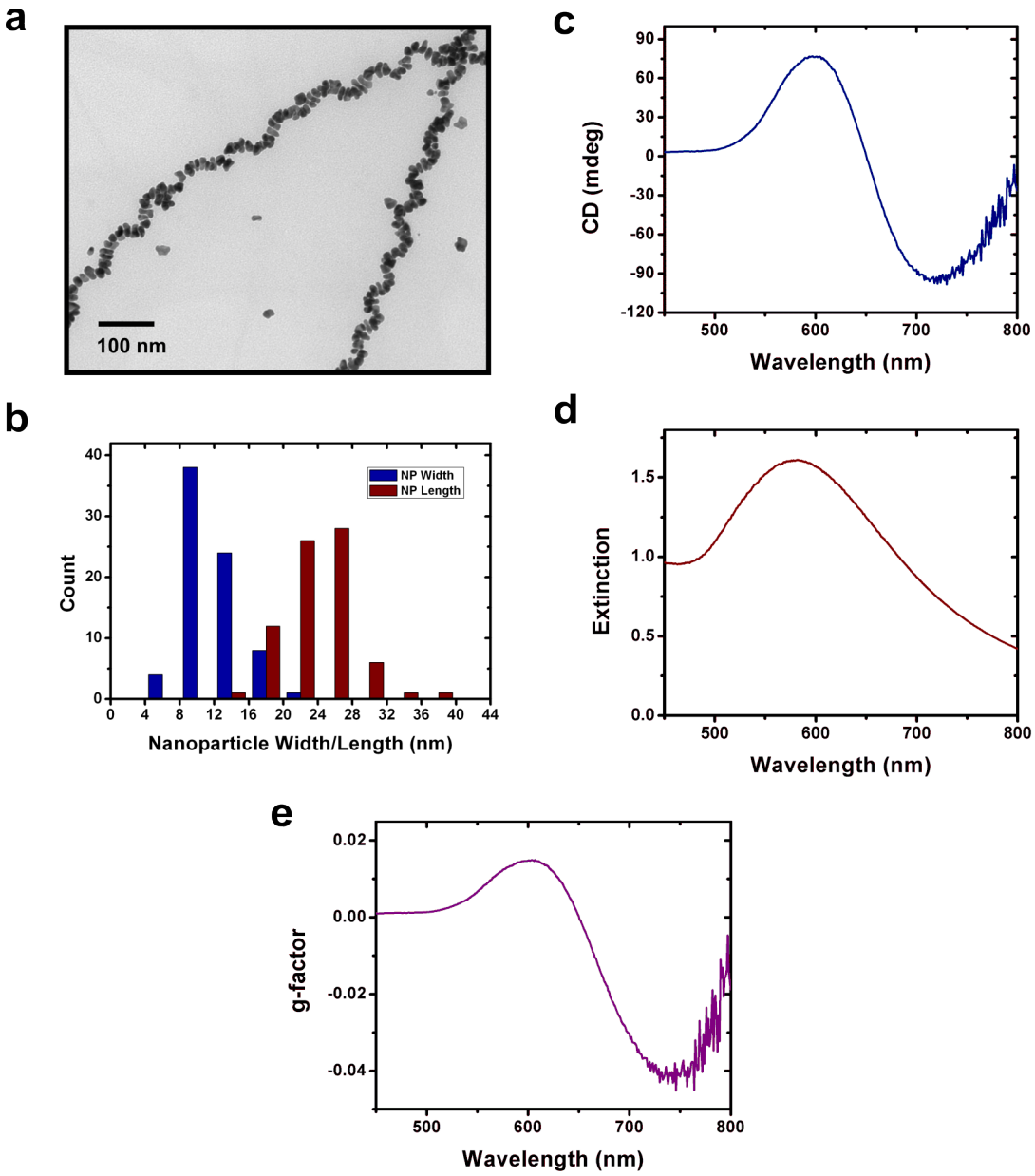

Figure S8. (a) TEM image of helices formed with 10 min. of sonication and 20 min. of incubation prior to $HAuCl_4$/TEAA addition. (b) The particle width and lengths were 12.1 ± 3.0 nm and 23.9 ± 3.9 nm, respectively (based on 75 counts, each). (c) CD spectrum of the optimized single helices exhibit a very strong CD signal. (d) UV-Vis extinction spectrum, and (e) g-factor graph showing absolute g-factor values up to 0.04. g-factor = Δε/ε, where Δε is the molar circular dichroism and ε is the molar extinctions.

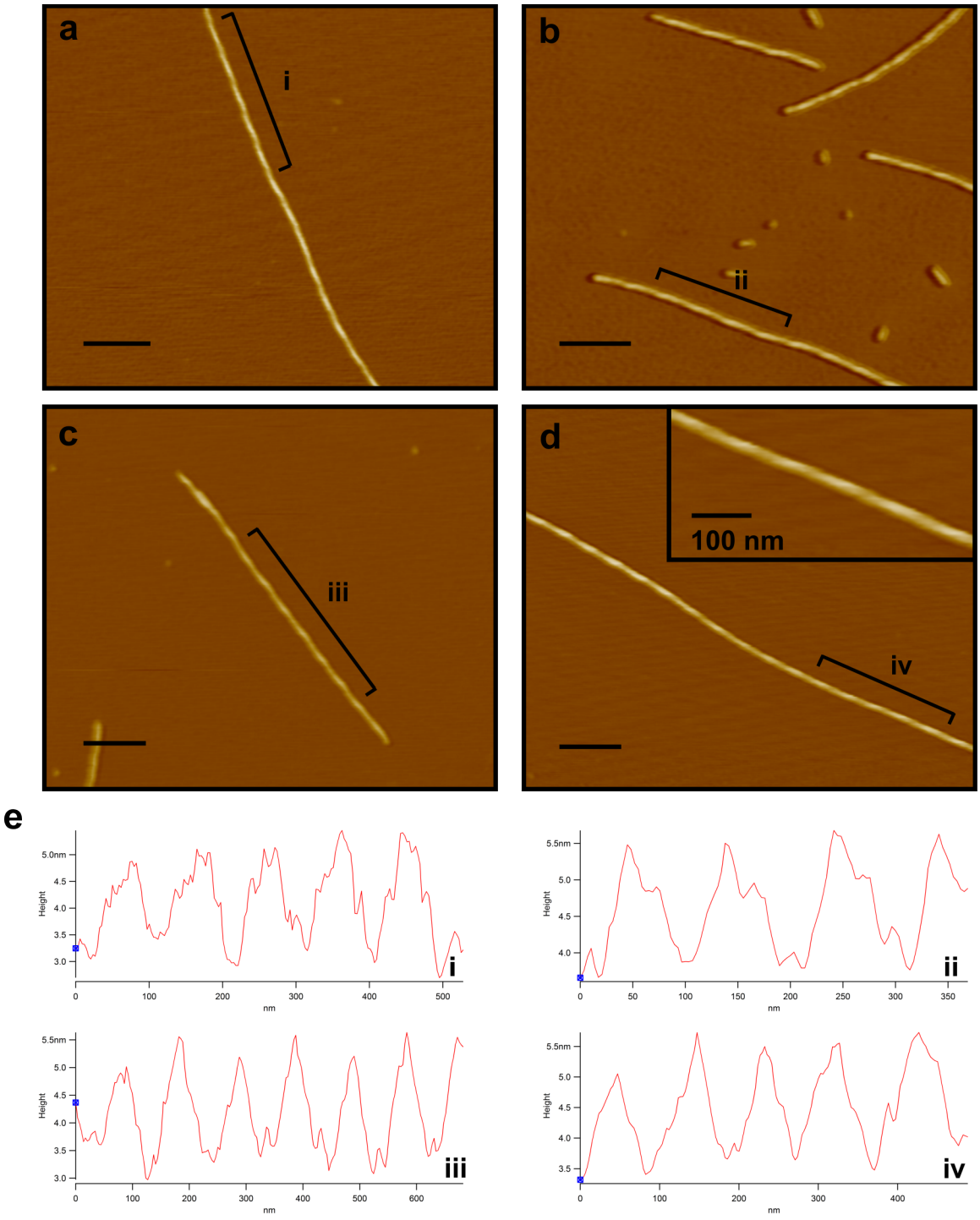

Figure S9. (a-d) AFM images of C_{18}-$(PEP_{Au}^{M\text{-}Ox})_2$ fibers dispersed on APTES-functionalized mica (scale bar = 200 nm) and (e) height traces of the labeled segments.

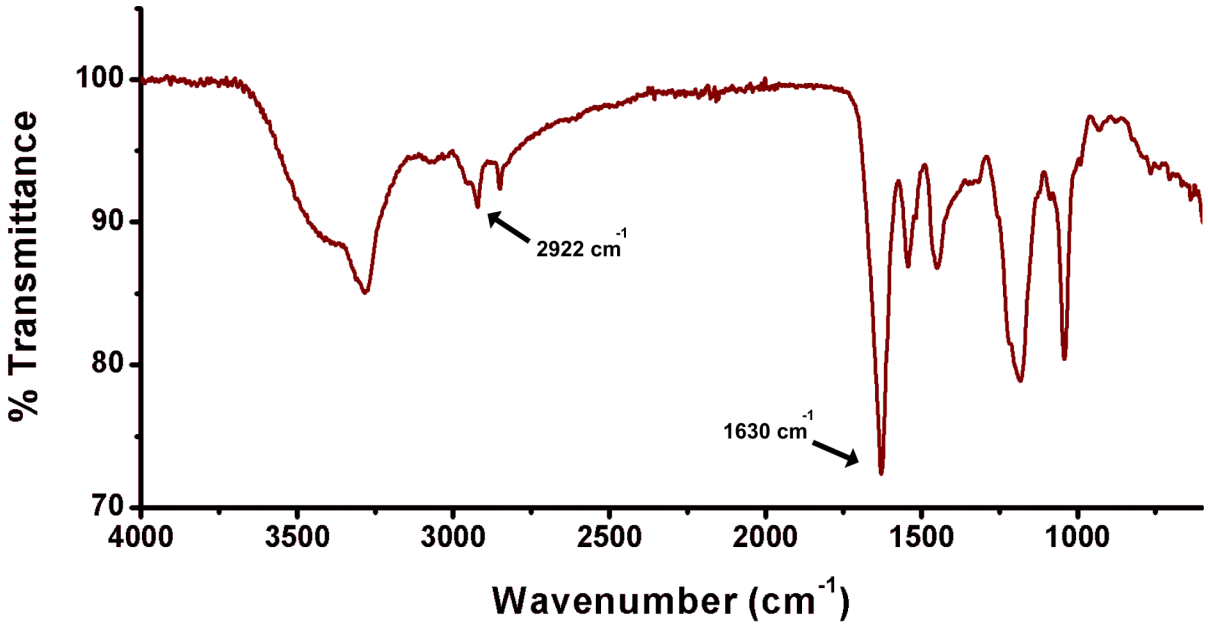

Figure S10. FTIR spectrum of C_{18}-($PEP_{Au}^{M\text{-}Ox}$)$_2$ fibers. Peaks at 1630 cm^{-1} and 2922 cm^{-1} correspond to the amide I band and C-H stretch, respectively.

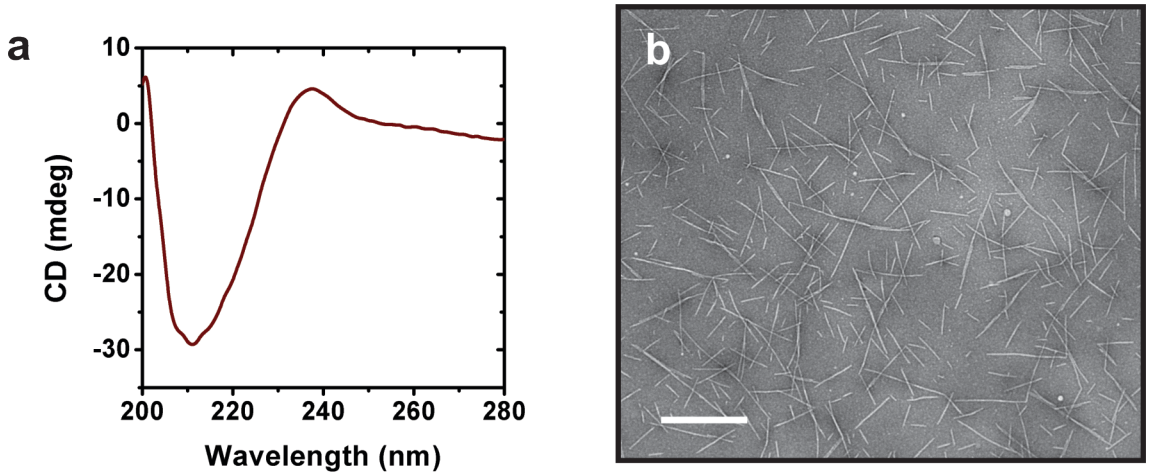

Figure S11. (a) CD spectrum of C_{18}-($PEP_{Au}^{M\text{-}Ox}$)$_2$ in 10 mM HEPES and 1 mM $CaCl_2$ after one day, and (b) corresponding negative stained TEM image (scale bar = 500 nm).

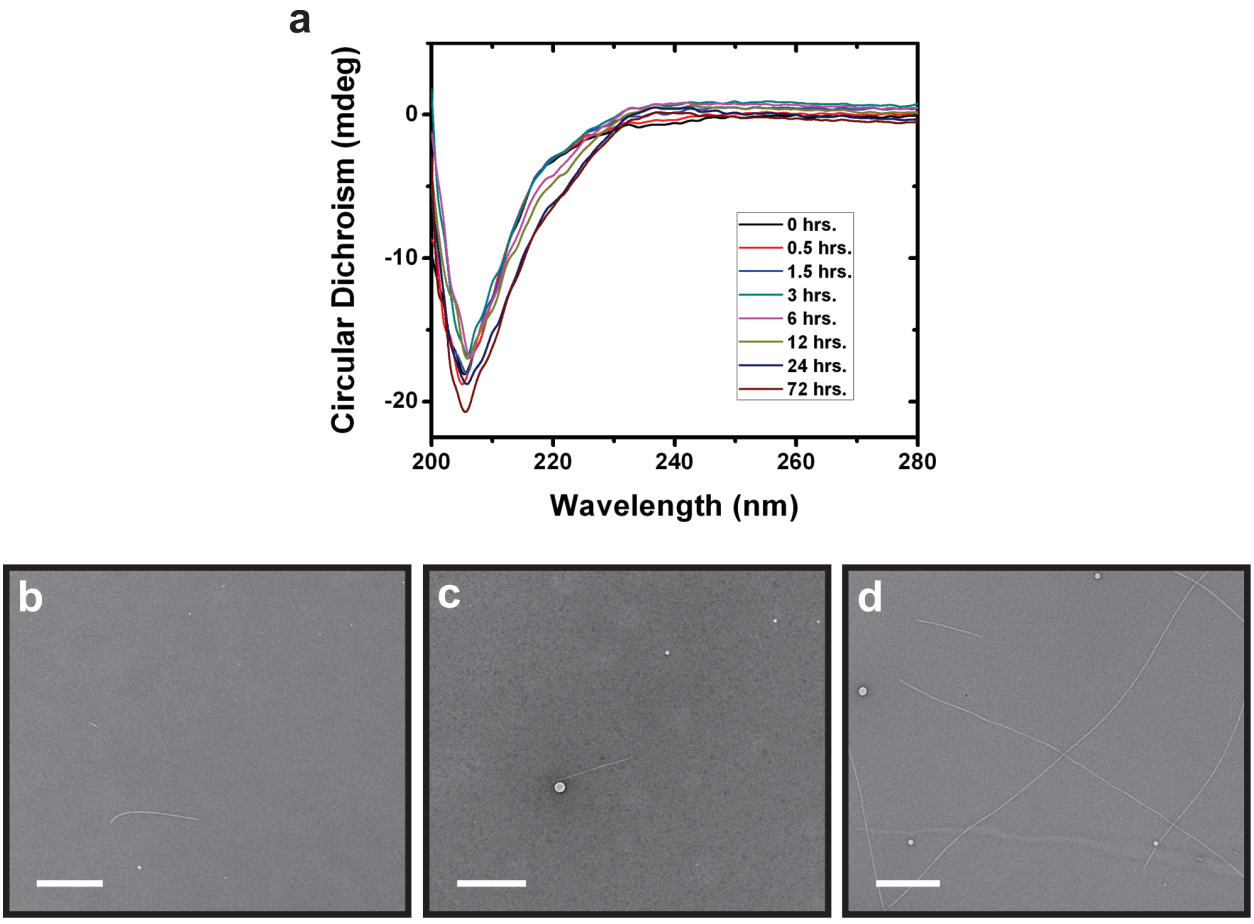

Figure S12. (a) CD spectra of C_{18}-($PEP_{Au}^{M\text{-}Ox}$)$_2$ in 10 mM HEPES as a function of time. Negative stained TEM images after (b) 15 min., (c) 3 hrs., and (d) 72 hrs. are shown (scale bar = 500 nm). Under these conditions, fibers form very slowly, and very few fibers are observed at early time points.

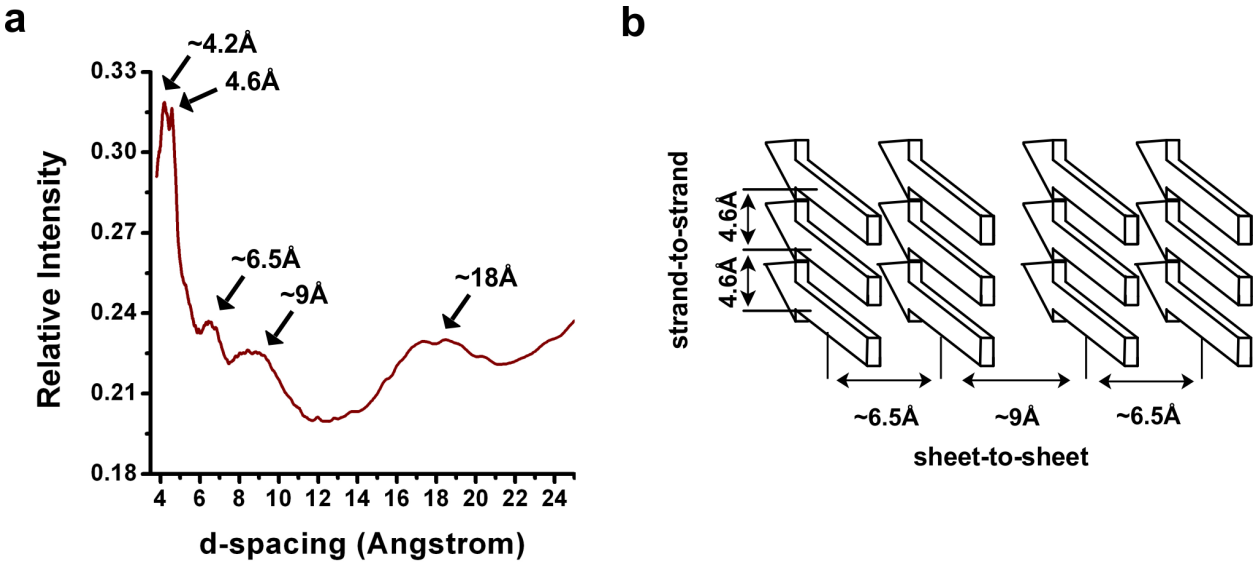

Figure S13. (a) Integrated d-spacings of the XRD diffractogram. (b) Figure showing the strand-to-strand and sheet-to-sheet distances as revealed via XRD.

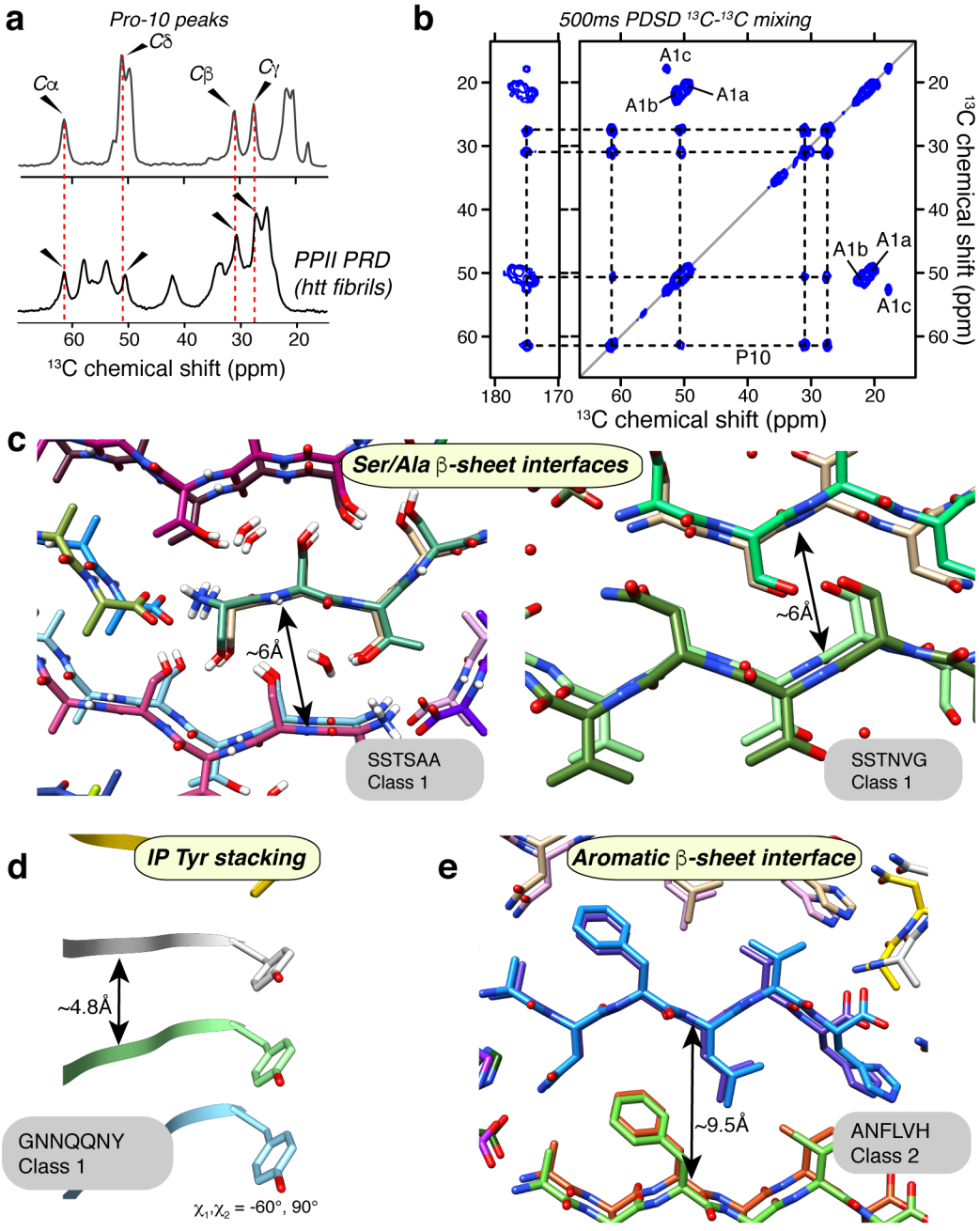

Figure S14. Additional ssNMR results and structural reference. (a) Aliphatic ^{13}C 1D MAS ssNMR spectrum of the site-specifically labeled C_{18}-$(PEP_{Au}{}^{M\text{-}Ox})_2$ assemblies (top), with the P10 peaks indicated. Bottom: ssNMR spectrum of fibrillar huntingtin exon1-derived peptide $htt^{NT}Q_{30}P_{10}K_2$, with ^{13}C,^{15}N-labeled Pro P48 (Adapted from ref.[1]). In both cases the labeled Pro is part of a PPII helix that flanks the β-sheet amyloid core. (b) Long-mixing 500ms PDSD 2D

ssNMR spectrum on the labeled C_{18}-($PEP_{Au}^{M\text{-}Ox}$)$_2$ assemblies. Compared to the short-mixing spectrum (Figure 5b) only new intra-residue P10 peaks are observed, with no contacts between the distinct A1 conformers. (c) Compact zipper interfaces mediated by Ser and other small amino acids in amyloid-like crystals of peptides SSTSAA and SSTNVG from RNase and IAPP.[2] The compact 6 Å inter-sheet distance is indicated. (d) Tyr ring stacking in GNNQQNY in-register parallel (IP) β-sheets.[3] (e) Amyloid interfaces featuring aromatic residues generate wider 9-10 Å inter-sheet distances. Illustrated for Phe in this Class-2 amyloid-like crystal of peptide ANFLVH.[4] The PDB entries for the four peptide crystal structures are 2ONW, 3DG1, 1YJP, and 5E5X.

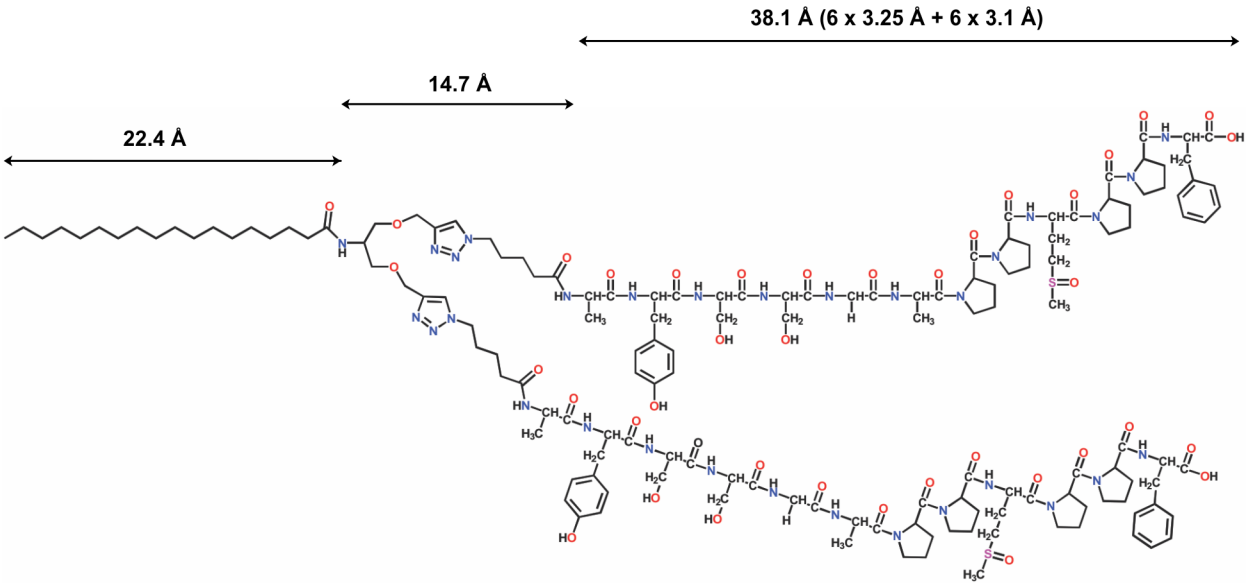

Figure S15. Length of the different extended segments of C_{18}-($PEP_{Au}^{M\text{-}Ox}$)$_2$. The total length of the extended molecule is ~7.5 nm. The length measurement of the peptide portion takes into account the average length spanned by one amino acid in both the parallel β-sheet (3.25 Å)[5] and the PPII (3.1 Å)[6] secondary structure.

Table S1. Detailed experimental conditions of the MAS ssNMR experiments. *Abbreviations: NS, number of scans; Set Temp, set temperature of cooling gas; MAS, magic angle spinning rate; RD, recycle delay; TPPM, two-pulse phase-modulated ^{1}H decoupling power during evolution and acquisition ; t_1 evol., number of evolution time increments and increment size in the indirect dimension.*

Figure	Expt.	NS	Set Temp (K)	MAS (kHz)	RD (s)	TPPM (kHz)	t_1 evol. (µs)	DARR mixing time (ms)	^{1}H-^{13}C Contact time (ms)
5b	2D ^{13}C-^{13}C CP-DARR	64	277	10	3	83	562*35.6	20	2
S14-a	^{1}H-^{13}C CP	1024	277	10	3	83	NA	NA	2
S14-b	2D ^{13}C-^{13}C PDSD	64	277	10	3	83	562*33.11	500	2

References

1. Hoop, C. L.; Lin, H.-K.; Kar, K.; Hou, Z.; Poirier, M. A.; Wetzel, R.; van der Wel, P. C. A. *Biochemistry* **2014,** *53* (42), 6653-6666.
2. Sawaya, M. R.; Sambashivan, S.; Nelson, R.; Ivanova, M. I.; Sievers, S. A.; Apostol, M. I.; Thompson, M. J.; Balbirnie, M.; Wiltzius, J. J. W.; McFarlane, H. T.; Madsen, A. O.; Riekel, C.; Eisenberg, D. *Nature* **2007,** *447* (7143), 453-457.
3. Nelson, R.; Sawaya, M. R.; Balbirnie, M.; Madsen, A. O.; Riekel, C.; Grothe, R.; Eisenberg, D. *Nature* **2005,** *435* (7043), 773-778.
4. Soriaga, A. B.; Sangwan, S.; Macdonald, R.; Sawaya, M. R.; Eisenberg, D. *The Journal of Physical Chemistry B* **2015**.
5. Nesloney, C. L.; Kelly, J. W. *Bioorganic & Medicinal Chemistry* **1996,** *4* (6), 739-766.
6. Adzhubei, A. A.; Sternberg, M. J. E.; Makarov, A. A. *Journal of Molecular Biology* **2013,** *425* (12), 2100-2132.